

# Dynamical Instability in Boolean Networks as a Percolation Problem

Shane Squires,\* Edward Ott, and Michelle Girvan

University of Maryland—College Park

(Dated: February 6, 2022)

Boolean networks, widely used to model gene regulation, exhibit a phase transition between regimes in which small perturbations either die out or grow exponentially. We show and numerically verify that this phase transition in the dynamics can be mapped onto a static percolation problem which predicts the long-time average Hamming distance between perturbed and unperturbed orbits.

Boolean networks have been a prominent tool for modeling gene regulation since their introduction by Kauffman in 1969 [1, 2]. In a Boolean network, each node is assigned a state, 0 or 1, which is synchronously updated at discrete time steps according to a pre-assigned update function which depends on the states of that node's inputs on the previous time step. When used to model gene regulatory networks, each node represents a gene, and the state of the node indicates whether or not the gene is being expressed. Kauffman's original considered random networks and update functions in which each of the  $N$  nodes has  $K$  input links from randomly chosen nodes (the  $N$ - $K$  model). Kauffman found numerically that when the in-degree  $K$  crosses a critical value, there is a transition between a stable phase, in which small perturbations die out, to an unstable phase, in which small perturbations grow and become macroscopic.

A derivation of the critical in-degree was given by Derrida and Pomeau for annealed  $N$ - $K$  networks [3]. Here “annealed” means that the network edges and update functions are randomly redrawn between time steps. They hypothesized that for large networks the stability properties of the annealed system are similar to those of the original frozen (non-annealed) system. This hypothesis is well-supported by numerical experiments [3, 4], and we refer to it as the “annealed approximation.” Recent work [5] has extended this approach by using a partial randomization, in which only the update functions (but not the network topology) are randomly generated at each time step. In contrast with the annealed approximation, this “semi-annealed” approximation describes the dynamics on a fixed network which may have non-trivial topological features such as edge assortativity [6], motifs [7], and community structure [8]. The only necessary assumption is that the network is locally treelike (it cannot have many short loops) [9].

Some recent papers have derived stability properties of Boolean networks without annealing [10, 11]. These papers are complementary to ours in the following sense. Although rigorous, their results only apply to the ensemble average of random networks with restrictions on their network topology and/or update functions. In contrast, because our results rely on the semi-annealed approximation, they can model the dynamics of a specific network.

Here, using our semi-annealed approach, we map the

*dynamical* problem of stability on a Boolean network onto the *static* problem of network percolation in the  $N \rightarrow \infty$  limit. Previous authors have discussed the percolation properties of the “frozen component” of  $N$ - $K$  networks [12–14], and others have used percolation to discuss the stability of  $N$ - $K$  lattices [15, 16]. In contrast, we show that a dynamic quantity, the long-time average Hamming distance between two initially close trajectories on a Boolean network, can be mapped onto the size of the giant out-component in a percolation problem. We will illustrate this map in three different contexts. First, we consider the well-known annealed approximation and map it onto percolation in the configuration model [17]. Second, we give a similar map from the semi-annealed approximation [5] to weighted site percolation [18]. Finally, we treat a more general class of update functions by mapping to a correlated bond percolation problem.

*Model:* A Boolean network is a directed network of  $N$  nodes, in which each node  $i$  is assigned a state,  $x_i(t) = 0$  or  $x_i(t) = 1$ , at each discrete time step  $t$ . We denote the in- and out-degrees of node  $i$  by  $d_i^{\text{in}}$  and  $d_i^{\text{out}}$  and the set of inputs to node  $i$  by  $\mathcal{J}_i$ . A Boolean function or “truth table”  $F_i$ , fixed in time, updates the state of each node  $i$  at each time step  $t$ ,  $x_i(t) = F_i(\{x_j(t-1) : j \in \mathcal{J}_i\})$ .

In the literature, the truth tables  $F_i$  are usually generated randomly (e.g., [3]). For each combination of input states to node  $i$ , the value of  $F_i$  is assigned to be 1 with probability  $p$  or 0 with probability  $1 - p$ , where  $p$  is the “bias probability.” Below, as in [5], we will consider the more general case where each  $F_i$  is generated with a different bias  $p_i$  assigned to each node  $i$ . Later, we will also consider the case of “canalizing” functions, in which one input acts as a master switch for the truth table. That is, input  $j$  to node  $i$  is canalizing if there is a state of  $x_j$  which completely determines the value of  $F_i$  independent of the other inputs to  $i$ . (When  $x_j$  is not equal to its canalizing value,  $F_i$  depends on the states of its other inputs.) Canalizing functions are thought to be common in real gene networks [19, 20].

Consider two trajectories,  $\mathbf{x}(t)$  and  $\tilde{\mathbf{x}}(t)$ , which evolve on the same Boolean network. The initial conditions  $\mathbf{x}(0)$  and  $\tilde{\mathbf{x}}(0)$  differ only on a small randomly chosen fraction  $\varepsilon$  of nodes. We say that a node  $i$  is “damaged” at time  $t$  if  $x_i(t) \neq \tilde{x}_i(t)$ , and our goal is to predict the extent of the damage at long times. Let  $y_i$  be the fraction of

time that node  $i$  is damaged on an orbit of length  $T$  as  $T \rightarrow \infty$ . The normalized long-time average Hamming distance  $Y = \langle y_i \rangle$ ,  $0 \leq Y \leq 1$ , is used as the order parameter for the stability phase transition. The average  $\langle \cdot \rangle$  is taken over all nodes  $i$ , then over all initial conditions which differ on a fraction  $\varepsilon$  of the nodes.

*Analytic Results:* First we treat the annealed approximation for random networks [21]. We assume that the truth tables are randomly generated with a bias which depends only on degree. Let  $P_{jk}$  be the probability that a node has  $j$  inputs and  $k$  outputs, and let the bias of such a node be  $p_{jk}$ . We define the sensitivity [22] to be  $q_{jk} = 2p_{jk}(1 - p_{jk}) \in [0, 1]$ , which can be interpreted as the probability that a node with  $j$  inputs and  $k$  outputs will become damaged at time  $t$  if at least one of its inputs is damaged at time  $t - 1$ .

In the annealed approximation,  $Y$  can be predicted analytically using a method derived in [3] and [23], which can be explained as follows. Let  $z$  denote the average degree of the network, i.e.  $z = \sum_{j,k} jP_{jk} = \sum_{j,k} kP_{jk}$ , and let  $E$  denote the probability that a randomly selected edge originates from a damaged node. A randomly selected edge originates from a node with  $j$  inputs and  $k$  outputs with probability  $\frac{kP_{jk}}{z}$ , and such a node will become damaged with probability  $q_{jk}$  if it has at least one damaged input, which occurs with probability  $1 - (1 - E)^j$ . Therefore,

$$\begin{aligned} E &= \sum_{j,k} \frac{kP_{jk}}{z} q_{jk} \left[ 1 - (1 - E)^j \right], \\ Y &= \sum_{j,k} P_{jk} q_{jk} \left[ 1 - (1 - E)^j \right]. \end{aligned} \quad (1)$$

In the stable regime, these equations only have the trivial solution  $E = 0$  and  $Y = 0$ , but there will be a nonzero solution in the unstable regime [23].

We now show that Eq. (1) can be mapped onto the generating function formalism for treating weighted site percolation in directed configuration-model networks, as developed in [17] and [24]. In this model, each node is deleted with some probability which depends only on its degree. The resulting ensemble of site-deleted networks exhibits a percolation phase transition, above which there is a macroscopic connected component or “giant component.” This giant component contains a core of mutually path-connected nodes called the giant strongly connected component (GSCC); this, along with all the nodes which can be reached from it, is called the giant out-component (GOUT). In our map, we will identify the probability that a node is *not* deleted with the sensitivity, writing  $q_{jk}$  for the probability that a node with  $j$  inputs and  $k$  outputs is undeleted. With this identification, we will show that  $Y$  maps onto the expected fraction of nodes in GOUT, which we denote  $S$ .

It is shown in [17] and [24] that  $S$  can be found as follows. First, define generating functions for the in-

degrees of nodes and edges,  $F_0(w) = \sum_{j,k} P_{jk} q_{jk} w^j$  and  $F_1(w) = \sum_{j,k} \frac{kP_{jk}}{z} q_{jk} w^j$ . Next, let  $u$  be the probability that a randomly selected edge is not in GOUT. The authors show through diagrammatic expansion that

$$\begin{aligned} u &= 1 - F_1(1) + F_1(u), \\ S &= F_0(1) - F_0(u). \end{aligned} \quad (2)$$

We note that the substitutions  $E = 1 - u$  and  $Y = S$  map Eq. (1) onto Eq. (2). Therefore, the phase transition between dynamical stability and instability in this ensemble of random Boolean networks is equivalent to the static percolation phase transition on the same ensemble.

Our second result is a more general derivation of the same correspondence, using the framework of [5]. This framework applies to a *specific* locally treelike network in which each node  $i$  can have its own arbitrarily chosen bias  $p_i$ , with an associated sensitivity  $q_i = 2p_i(1 - p_i)$ . Again, we will identify the sensitivity  $q_i$  with a site nondeletion probability and map the Hamming distance,  $Y$ , onto the size of GOUT,  $S$ . We begin by writing an analogue of Eq. (1) for a specific node in a semi-annealed, locally treelike Boolean network,

$$y_i = q_i \left[ 1 - \prod_{j \in \mathcal{J}_i} (1 - y_j) \right]. \quad (3)$$

This is the long-time limit of a damage-spreading equation derived in [5], which noted that  $i$  will become damaged with probability  $q_i$  if at least one of its inputs is damaged. The assumption that the network is locally treelike is necessary because all the probabilities in the product are treated as independent.

Reference [18] derives a similar condition for site percolation on locally treelike directed networks in which the probability that each node is *not* deleted is  $q_i$ . It defines  $\eta_i$  as the fraction of site-deleted networks for which node  $i$  is *not* in GOUT, and it shows that

$$\eta_i = 1 - q_i + q_i \prod_{j \in \mathcal{J}_i} \eta_j, \quad (4)$$

because a node is not in GOUT when it is either deleted or has no inputs from GOUT. We note that substituting  $y_i = 1 - \eta_i$  maps Eq. (3) onto Eq. (4). Because  $Y = \langle y_i \rangle$  and  $S = \langle 1 - \eta_i \rangle$ , this map also yields  $Y = S$ . For  $S$ , the average  $\langle \cdot \rangle$  is first taken over all nodes  $i$ , then over all node deletion trials.

We now introduce a third case, in which we consider Boolean networks with canalizing functions. The method used for our previous results can be extended to canalizing functions, but because the truth table elements in a canalizing function are not generated independently, we need to consider a new type of percolation problem which we call correlated bond percolation. Instead of typical bond percolation, in which each bond is occupied

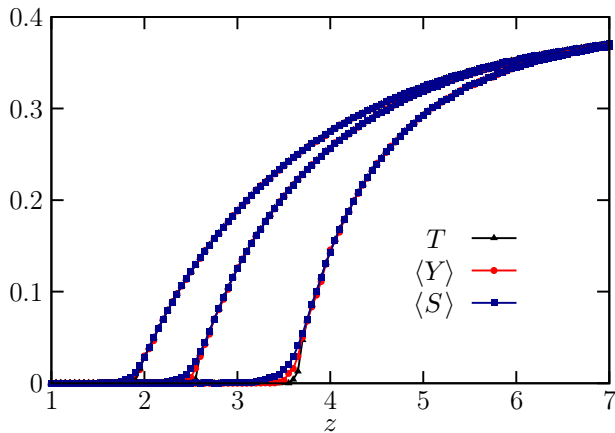


FIG. 1 (color online). The ensemble averages of  $Y$ ,  $S$ , and  $T$  (taken over 20 networks) versus the average degree  $z$ , for three families of networks. The three families of networks are assortative (left), neutral (middle), and disassortative (right).

or deleted independently, we consider joint probabilities where the deletion of two bonds may be correlated if they are inputs to the same node.

Here we describe a correlated bond percolation problem that corresponds to a Boolean network whose truth tables each have one canalizing input but are otherwise generated randomly. That is, for each node  $i$ , there is a canalizing input  $c_i$ , and all the rows of the truth table on which  $x_{c_i}$  assumes its canalizing value have the same constant output; but the outputs of the other rows are randomly generated with a probability bias  $p_i$ . To begin, we imagine that the system is equally likely to be in any of its states. As we will show, it is then formally possible to obtain equations describing damage spreading in closed form. Based on our numerical results, we conjecture that these equations can be used to predict damage spreading in a large class of Boolean networks with frozen truth tables.

Working under the supposition that all system states are equally probable, we now derive an expression for  $y_i$ . Let  $r_i$  denote the “activity” of  $c_i$  on  $i$  [22], defined as the fraction of states in which  $i$  will become damaged if  $c_i$  becomes damaged. If  $c_i$  is not damaged, it may be in either the canalizing or non-canalizing state, each with probability  $\frac{1}{2}$ . In the first case it is impossible for  $i$  to become damaged, while the second case is equivalent to Eq. (3). Therefore,

$$y_i = r_i y_{c_i} + \frac{1}{2} q_i (1 - y_{c_i}) \left[ 1 - \prod_{j \in \mathcal{J}'_i} (1 - y_j) \right], \quad (5)$$

where  $\mathcal{J}'_i = \mathcal{J}_i - \{c_i\}$  and  $q_i$  is the sensitivity of the half of the truth table where  $x_{c_i}$  is not in its canalizing state.

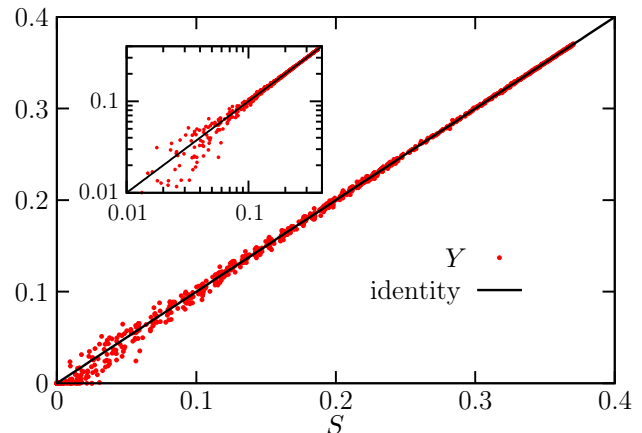


FIG. 2 (color online).  $Y$  versus  $S$  for individual neutrally assortative networks.

It can be shown that this is equivalent to

$$\eta_i = 1 - r_i + \left( r_i - \frac{1}{2} q_i \right) \eta_{c_i} + \frac{1}{2} q_i \prod_{j \in \mathcal{J}_i} \eta_j, \quad (6)$$

where  $\eta_i = 1 - y_i$ . This corresponds to a correlated bond percolation problem in which one of the following three things may occur. With probability  $1 - r_i$ , all edges to  $i$  are deleted; with probability  $r_i - \frac{1}{2} q_i$ , all of  $i$ 's edges are deleted except for the edge from  $c_i$ ; and otherwise no input edges are deleted. Note that it is straightforward to describe the case where only some of the nodes have a canalizing input by using Eqs. (5-6) for those nodes and Eqs. (3-4) for the others.

*Numerical Results:* We begin with the map described by Eqs. (3-4), since it is more general than Eqs. (1-2). We compare the long-time average Hamming distance  $Y$  to the size of the giant out-component  $S$  for particular networks. We also compare both  $Y$  and  $S$  to the theoretical prediction given by the solution to Eq. (3), which we denote  $T$ .

Our algorithm is as follows. First we create a configuration-model network with  $N = 10^5$  nodes. The data in the figures were obtained using networks with Poisson-distributed in-degrees and scale-free out-degrees; we have also tested other degree distributions and found similar results. If desired, we then enhance interesting topological features such as assortativity or feedforward loops using the same algorithms as in [5]. Next, we assign each node a bias  $p_i$ . These may be distributed randomly, or, if we wish to encourage (impede) instability on the network, we distribute them so that the nodal average  $\langle q_i d_i^{\text{in}} d_i^{\text{out}} \rangle$  is maximized (minimized) [5]. For the data in the figures, the biases  $p_i$  were distributed randomly so that the sensitivities  $q_i$  form a uniform distribution on the interval  $[.3, .5]$ . We choose random initial conditions for  $\mathbf{x}$ , and a randomly selected fraction  $\varepsilon = .01$  of the nodes are flipped for the initial conditions of  $\tilde{\mathbf{x}}$ .

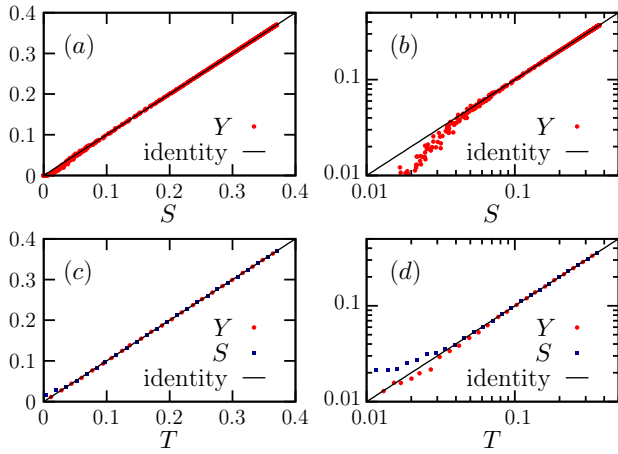


FIG. 3 (color online). (a) Linear and (b) log-log scatterplots of  $Y$  versus  $S$  for data generated in the same way as that of Fig. 2, except that now we average over the quenched disorder in the truth tables as described in the text. (c) Linear and (d) log-log scatterplots of  $Y$  and  $S$  versus  $T$  for the same data, sampling alternate points for visibility.

To find  $Y$ , we time-evolve the system and average  $|x_i(t) - \tilde{x}_i(t)|$  between  $t = 900$  and  $t = 1000$ , averaging over 100 initial conditions. The theoretical prediction is found by iterating Eq. (3) until it converges to a solution  $\hat{\mathbf{y}}$ , then taking  $T = \langle \hat{y}_i \rangle$ . Finding  $S$  is less straightforward, because a typical percolation problem is only guaranteed to have a single, well-defined giant out-component in the  $N \rightarrow \infty$  limit. For reasons discussed in the online Supplemental Material, we choose the following procedure. We delete each node  $i$  with probability  $1 - q_i$  and find any strongly connected components (SCCs) in the resulting network, where we define an SCC to be a mutually path-connected set of nodes containing at least one loop. We define  $S$  to be the fraction of nodes which can be reached from at least one SCC, averaged over the ensemble of deletion trials. We average  $10^3$  deletion trials per network. We find that the numerical uncertainty in our measured values of  $T$ ,  $Y$ , and  $S$  for each point in Figs. 1–4 is smaller than the point size; see the Supplemental Material for details.

Figure 1 illustrates the relationship between  $Y$ ,  $S$ , and  $T$  for networks generated in this way. We see that  $Y$  and  $S$  have the same average values on the ensemble of random networks with given average degree  $z$ . However, in Fig. 2, we see that the prediction  $Y = S$  sometimes fails for individual networks, especially near the phase transition. The deviations in Fig. 2 are primarily caused by the quenched disorder in the truth tables, which may cause orbits to fall onto attractors which visit only a small fraction of the state space (and so may deviate from the semi-annealed approximation).

In Fig. 3, we have averaged over this quenched disorder by choosing truth tables from an ensemble of closely

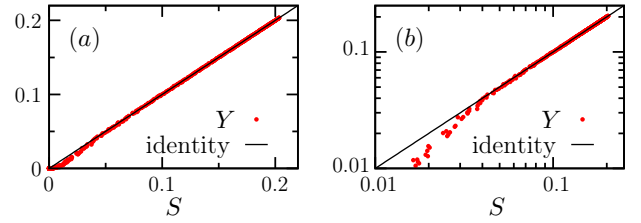


FIG. 4 (color online). Scatterplots of  $Y$  versus  $S$  for networks in which each node has one canalizing input, using Eqs. (5-6).

related frozen truth tables (but not networks) as follows. Before we time-evolve each new pair of initial conditions, we perform a set of exchanges on the truth tables. For each edge  $j \rightarrow i$ , with probability  $\frac{1}{2}$ , we exchange  $x_j = 0$  and  $x_j = 1$  on the truth table for  $i$ . We note that there are two major differences between this and the semi-annealed approximation. In the latter, the truth tables are changed *during* the dynamics, whereas here they are only changed before each new dynamical trial. Second, whereas the semi-annealed approximation treats all inputs interchangeably, this procedure preserves input-specific information (such as whether an input is canalizing). In Fig. 3, we see that this procedure yields excellent agreement between  $Y$ ,  $S$ , and  $T$  for individual networks well above the transition. Near the transition and below it, finite-size effects still cause  $S$  (and, to a lesser extent,  $Y$ ) to deviate slightly from the prediction  $T$ . These effects are discussed in the Supplemental Material.

In Fig. 4, we perform the same numerical experiment for the case in which each node has one canalizing input. We find that  $Y$ ,  $S$ , and  $T$  agree for individual networks when we use the map between Eqs. (5) and (6), but the map between Eqs. (3) and (4) fails for this case, indicating that we retain significant input-specific information about the dynamics when we average over the quenched disorder in the truth tables.

*Discussion:* We have presented evidence that the stability of a Boolean network can be understood in terms of a related percolation problem on that network. This relationship may be helpful in understanding the stability of systems modeled by Boolean networks, such as gene regulatory networks and neural networks. Two previously-studied cases (the annealed and semi-annealed approximations) map onto known results for percolation, and a case of biological interest (canalizing truth tables) maps onto a novel percolation problem. These maps are valid for the typical cases in the literature (large, locally tree-like networks with random or canalizing truth tables), but have the advantage of applying to specific networks rather than ensembles of random networks. Numerical experiments show excellent agreement with our analysis when averaged over a family of quenched truth tables.

*Acknowledgements:* This work was funded by ONR grant N000140710734 and ARO grant W911NF1210101.

---

\* squires@umd.edu

- [1] S. A. Kauffman, J. Theor. Biol. **22**, 437 (1969).
- [2] H. de Jong, J. Comp. Biol. **9**, 67 (2002).
- [3] B. Derrida and Y. Pomeau, Europhys. Lett. **1**, 45 (1986).
- [4] U. Bastolla and G. Parisi, Physica D **98**, 1 (1996).
- [5] A. Pomerance et al., Proc. Natl. Acad. Sci. **106**, 8209 (2009).
- [6] S. Maslov and K. Sneppen, Science **296**, 910 (2002).
- [7] R. Milo et al., Science **298**, 824 (2002).
- [8] Q. Cui et al., Mol. Sys. Biol. **3** (2007).
- [9] The locally treelike approximation is discussed in detail in [5] and [18]. Configuration-model random networks with finite average degree are locally treelike as  $N \rightarrow \infty$  [17]. It is quite common for treelike approximations to give excellent results even when the underlying network has significant clustering [25]; this was observed for Boolean networks in [5].
- [10] A. Mozeika and D. Saad, Phys. Rev. Lett. **106**, 214101 (2011).
- [11] C. Seshadhri et al., Phys. Rev. Lett. **107**, 108701 (2011).
- [12] H. Flyvbjerg, J. Phys. A **21**, L955 (1988).
- [13] T. Mihaljev and B. Drossel, Phys. Rev. E **74**, 046101 (2006).
- [14] B. Samuelsson and J. E. S. Socolar, Phys. Rev. E **74**, 036113 (2006).
- [15] A. Hansen, J. Phys. A **21**, 2481 (1988).
- [16] S. P. Obukhov and D. Stauffer, J. Phys. A **22**, 1715 (1989).
- [17] M. E. J. Newman, S. H. Strogatz, and D. J. Watts, Phys. Rev. E **64**, 026118 (2001).
- [18] J. G. Restrepo, E. Ott, and B. R. Hunt, Phys. Rev. Lett. **100**, 058701 (2008).
- [19] S. E. Harris et al., Complexity **7**, 23 (2002).
- [20] S. Kauffman, C. Peterson, B. Samuelsson, and C. Troein, PNAS **100**, 14796 (2003).
- [21] B. Luque and R. V. Solé, Phys. Rev. E **55**, 257 (1997).
- [22] I. Shmulevich and S. A. Kauffman, Phys. Rev. Lett. **93**, 048701 (2004).
- [23] D. Lee and H. Rieger, J. Theor. Biol. **248**, 618 (2007).
- [24] D. S. Callaway et al., Phys. Rev. Lett. **85**, 5468 (2000).
- [25] S. Melnik et al., Phys. Rev. E **83**, 036112 (2011).